#### ORIGINAL ARTICLE



# Recovery of rapidly decaying source terms from dynamical samples in evolution equations

Akram Aldroubi<sup>1</sup> · Le Gong<sup>1</sup> D · Ilya Krishtal<sup>2</sup>

Received: 2 September 2022 / Accepted: 3 April 2023 © The Author(s), under exclusive licence to Springer Nature Switzerland AG 2023

#### **Abstract**

We analyze the problem of recovering a source term of the form  $h(t) = \sum_j h_j \phi(t-t_j)$   $\chi_{[t_j,\infty)}(t)$  from space-time samples of the solution u of an initial value problem in a Hilbert space of functions. In the expression of h, the terms  $h_j$  belong to the Hilbert space, while  $\phi$  is a generic real-valued function with exponential decay at  $\infty$ . The design of the sampling strategy takes into account noise in measurements and the existence of a background source.

**Keywords** Sampling theory · Forcing · Frames · Reconstruction · Semigroups · Continuous sampling

Mathematics Subject Classification 46N99 · 42C15 · 94O20

#### 1 Introduction

Dynamical sampling refers to a set of problems in which a space-time signal u evolving in time under the action of a linear operator as in (1) below is to be sampled on a space-time set  $S = \{(x, t) : x \in X, t \in T\}$  in order to recover  $u_0, u, F$  or other information related to these functions. For example, when the goal is to recover  $u_0$ , we get the so called space-time trade-off problems (see e.g., [3, 5-7, 14, 15, 19, 26, 27]). If the goal is to recover the unknown underlying operator A, or some of its spectral characteristics, we get the system identification problem in dynamical sampling [9, 12, 25]. In other situations, the goal is to identify the driving source term from space-time samples [8, 11]. In all dynamical sampling problems, frame theory plays a fundamental albeit, at

Communicated by Mark Iwen.

Published online: 25 April 2023 

Birkhäuser

 <sup>□</sup> Le Gong le.gong@vanderbilt.edu

Department of Mathematics, Vanderbilt University, Nashville, USA

Department of Mathematical Sciences, Northern Illinois University, DeKalb, USA

15 Page 2 of 24 A. Aldroubi et al.

times, hidden role (see e.g. [4, 9, 10, 14]). Moreover, this important connection has also been used to develop frame theory and led to the concept of dynamical frames (see e.g. [1, 2, 13, 16–18, 21]). In this paper, we consider the problem of designing space-time sampling patterns that permit recovery of the source term of an initial value problem (IVP) or some relevant portion thereof.

#### 1.1 Motivation

In [8], the authors introduced a new sampling technique which prescribes how one may sample the solution of an IVP to detect "bursts" in the driving force of the system. The proposed special structure of the samplers allowed one to "predict" the value of the solution at the next sampling instance provided that no burst occurred during the sampling period. Thus, if the samples at the end of the period were significantly different from the prediction, a "burst" must have occurred. In [8], the "bursts" were modeled as a linear combination of Dirac measures. In this paper, we employ a modification of the same technique to detect localized non-instantaneous sources which decay exponentially in time after activation [22]. Such sources may describe, for example, an irregular intake of rapidly degrading substances. In particular, the IVP we consider may model a complex chemical reaction contaminated by such an intake, and our goal, in this case, would be to determine when and what substances were added to the system. Many other phenomena driven by natural mechanisms, such as the dispersion of pollution, the spreading of fungal diseases and the leakage of biochemical waste, can also be described by IVP with the source terms considered here (see [22–24] and references therein). Thus, a robust sampling and reconstruction algorithm for such IVP would be beneficial for studying these real-world applications.

## 1.2 Problem setting

Let us give a more precise description of our setting. We consider the following abstract initial value problem:

$$\begin{cases} \dot{u}(t) = Au(t) + F(t) \\ u(0) = u_0, \end{cases} \quad t \in \mathbb{R}_+, \ u_0 \in \mathcal{H}.$$
 (1)

Above, the function  $u: \mathbb{R}_+ \to \mathcal{H}$  is assumed to be almost everywhere differentiable with the derivative  $\dot{u} \in L^2(\mathbb{R}_+, \mathcal{H})$ , where  $\mathcal{H}$  is some Hilbert space of functions on a subset of  $\mathbb{R}^d$ . Additionally,  $F: \mathbb{R}_+ \to \mathcal{H}$  is a forcing term a portion of which we wish to recover and  $A: D(A) \subseteq \mathcal{H} \to \mathcal{H}$  is the generator of a strongly continuous semigroup  $T: \mathbb{R}_+ \to B(\mathcal{H})$ . We shall also occasionally use the notation u = u(x, t), where the variable  $x \in \mathbb{R}^d$  is the spatial variable and  $t \in \mathbb{R}_+$  represents time, with the understanding that for each fixed  $t \in \mathbb{R}_+$ ,  $u(\cdot, t)$  is a function in  $\mathcal{H}$ .

As in [8], we consider force terms of the form:

$$F = h + \eta$$

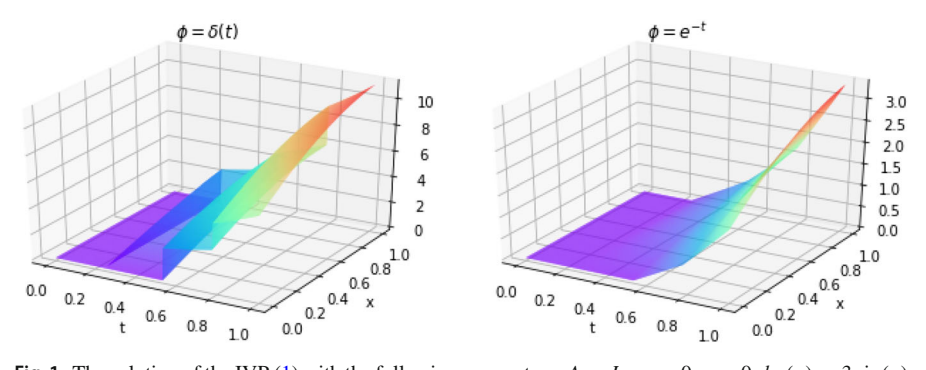


**Fig. 1** The solution of the IVP (1) with the following parameters: A = I,  $u_0 = 0$ ,  $\eta = 0$ ,  $h_1(x) = 3\sin(x)$ ,  $h_2(x) = 2.5\cos(x)$ ,  $h_3(x) = x + 2$ ,  $x \in [0, 1]$ , and  $t_1 = 0.25$ ,  $t_2 = 0.54$ ,  $t_3 = 0.78$ 

where  $\eta$  is a Lipschitz continuous background source term. Unlike [8], however, the burst-like forcing term h is assumed to be given by

$$h(t) = \sum_{j=1}^{N} h_j \phi(t - t_j) \chi_{[t_j, \infty)}(t),$$
 (2)

where  $0 < t_1 < \dots < t_N$ ,  $h_j \in \mathcal{H}$ , and  $\phi$  is a non-negative function with a certain prescribed decay on  $[0, \infty)$ . We regard  $t_j$  and  $h_j$  as the time and the shape of the j-th burst, respectively.

The goal of this paper is to provide an algorithm similar to one in [8] that recovers the "burst-like" portion h of F from space-time samples of the solution u of (1). Once again we shall choose the structure of the samplers that would allow one to detect an occurrence of a burst in a sampling period by comparing the predicted values of the samples with the actual samples. In fact, we will show that the same structure of samplers that was used in the first of the two approaches in [8] may also be used in the current situation. The recovery algorithms in this paper, however, are significantly different and are not just a straightforward tweak of the ones in [8]. The main difficulty in the current setting is the need to account for the influence of past bursts which was not an issue when those were Diracs.

To gain a visual understanding of these two cases, we set up a specific IVP with the two types of  $\phi$  and plot the respective graphs of u = u(x, t) in Fig. 1.

The model incorporating Dirac functions exhibited noticeable jumps when bursts happened, while the model with exponential decay is smoother, highlighting the challenges of detecting the bursts and mitigating the influence of past bursts.

## 1.3 Paper organization

The rest of the paper is organised as follows. In Sect. 2, we remind the reader of some basic properties of one-parameter operator semigroups and their use in solving IVP such as (1). We also list all model assumptions for the algorithms of this paper.

15 Page 4 of 24 A. Aldroubi et al.

In Sect. 3, we present the main results. The section is divided into two parts. In Sect. 3.1, the decay function  $\phi$  in (2) is assumed to be of the form  $e^{-\rho t}$  for some  $\rho > 0$ . We present the structure of measurement functions (5) for this case and utilize discrete samples of the measurement functions to approximate the burst time and shape in the presence of background source and measurement acquisition errors. In Sect. 3.2, we consider a more general model, where the decay function  $\phi$  does not have a concrete formula, but is rather bounded above by a decaying exponential function. Under additional assumptions that the shapes of the bursts are uniformly bounded and that the differences  $t_{j+1} - t_j$ , j = 1, ..., N - 1, are large enough, we present a modification of the algorithm from Sect. 3.1, which solves the same problem in this more general setting. Finally, in Sect. 4, we set up specific (synthetic) dynamical systems to test the algorithms and describe the results of the testing.

# 2 IVP solution and model assumptions

In this section, we recall a few basic facts from the theory of one-parameter operator semigroups and summarize our model assumptions.

#### 2.1 IVP toolkit

**Definition 2.1** A strongly continuous operator semigroup is a map  $T : \mathbb{R}_+ \to B(\mathcal{H})$  (where  $B(\mathcal{H})$  is the space of all bounded linear operators on  $\mathcal{H}$ ), which satisfies

- (i) T(0) = I,
- (ii) T(t+s) = T(t)T(s) for all  $t, s \ge 0$ , and
- (iii)  $||T(t)h h|| \to 0$  as  $t \to 0$  for all  $h \in \mathcal{H}$ .

**Proposition 2.2** [20] There exist constants  $a \in \mathbb{R}$  and  $M \ge 1$  such that

$$||T(t)|| < Me^{at}$$

for all  $t \geq 0$ .

Recall [20, p. 436] that the (mild) solution of (1) can be represented as

$$u(t) = T(t)u_0 + \int_0^t T(t-s)F(s)ds.$$
 (3)

Substituting  $F = h + \eta$  with h of the form (2) yields

$$u(t) = T(t)u_0 + \sum_{t_j < t} \int_{t_j}^t T(t - s)h_j \phi(s - t_j) ds + \int_0^t T(t - s)\eta(s) ds, \quad t \ge 0.$$
(4)

Birkhäuser 🖹

Content courtesy of Springer Nature, terms of use apply. Rights reserved.

In this paper, we will use the measurement function  $\mathfrak{m}: \mathbb{R}_+ \times \mathcal{H} \to \mathbb{R}$  given by

$$\mathfrak{m}(t,g) = \langle u(t), g \rangle + \nu(t,g), \ t \ge 0, \ g \in G, \tag{5}$$

where  $\langle \cdot, \cdot \rangle$  is the inner product in  $\mathcal{H}$ ,  $\nu$  is the measurement acquisition noise, and G is the collection of samplers whose structure we wish to prescribe.

## 2.2 Model assumptions

**Assumption 1** The set of samplers G has the form  $G = \widetilde{G} \cup T^*(\beta)\widetilde{G}$  for some countable (possibly, finite) set  $\widetilde{G} \subseteq \mathcal{H}$ . Additionally, in the model of Sect. 3.2, the set  $\widetilde{G}$  is assumed to be uniformly bounded by some  $R \in \mathbb{R}$ , i.e.  $R = \sup_{g \in \widetilde{G}} \|g\| < \infty$ .

**Assumption 2** In Sect. 3.2, the burst terms are uniformly bounded, i.e.  $||h_j|| \le H$ , j = 1, ..., N, for some  $H \in \mathbb{R}$ .

**Assumption 3** The background source  $\eta: \mathbb{R}_+ \to \mathcal{H}$  is uniformly bounded by a constant K > 0 and Lipschitz with a Lipschitz constant  $L \geq 0$ , i.e.  $\sup_{t \geq 0} \|\eta(t)\| \leq K$  and  $\|\eta(t+s) - \eta(t)\| \leq Ls$ ,  $t, s \in \mathbb{R}_+$ .

**Assumption 4** The additive noise v in the measurements (5) satisfies

$$\sup_{t>0,\ h\in\mathcal{H}}|\nu(t,h)|\leq\sigma.$$

**Assumption 5** (1) In Sect. 3.1 we assume that the distance between two bursts is bounded below:  $t_{j+1} - t_j \ge 4\beta$ .

(2) In Sect. 3.2 we assume  $t_{j+1} - t_j \ge D + 4\beta$  with some positive number D.

#### 3 Main results

## 3.1 Model with specific decay function

In this section, we consider the special case where the decay function  $\phi$  is given by  $\phi(t) = e^{-\rho t}$  with some  $\rho > 0$ :

$$\begin{cases} \dot{u}(t) = Au(t) + \sum_{j=1}^{N} h_{j} e^{-\rho(t-t_{j})} \chi_{[t_{j},\infty)}(t) + \eta(t) \\ u(0) = u_{0}. \end{cases}$$
 (6)

Since the operator A generates a strongly continuous semigroup T, by Proposition 2.2, we can find real numbers M and a satisfying  $||T(t)|| \le Me^{at}$  for all  $t \ge 0$ . We will use these numbers to estimate the accuracy of our recovery algorithm.

We acquire the following set of measurements:

$$\mathfrak{m}_n\left(\frac{g}{\beta}\right) = \left(u(n\beta), \frac{g}{\beta}\right) + \nu\left(n\beta, \frac{g}{\beta}\right),$$

🔊 Birkhäuser

15 Page 6 of 24 A. Aldroubi et al.

$$\mathfrak{m}_{n}\left(\frac{T^{*}(\beta)g}{\beta}\right) = \left\langle u(n\beta), \frac{T^{*}(\beta)g}{\beta} \right\rangle + \nu\left(n\beta, \frac{T^{*}(\beta)g}{\beta}\right), \quad g \in \widetilde{G}, n \in \mathbb{N}, \quad (7)$$

where  $\beta$  is the time sampling step,  $T^*(t)$  is the adjoint operator of T(t), and  $\nu$  represents an additive noise (see Assumption 4).

The first of the pair of measurements in (7) serves to assess the current state of the system whereas the second one will be used as a predictor of the measurement at  $t = (n + 1)\beta$ .

To explain our idea of the recovery algorithm, we first present what happens in the ideal case when the measurements are noiseless ( $\nu \equiv 0$ ) and there is no background source ( $\eta \equiv 0$ ). For the convenience of exposition, we define  $f_n \in \mathcal{H}$  and  $\tau_n \in [n\beta, (n+1)\beta)$  for each n as follows

$$\begin{cases} f_n = h_j, \ \tau_n = t_j, & \text{if the } j\text{-th burst occurred in } [n\beta, (n+1)\beta); \\ f_n = 0, \quad \tau_n = n\beta, & \text{if no burst occurred in } [n\beta, (n+1)\beta). \end{cases}$$
(8)

There is no ambiguity in the above definition due to Assumption 5.

To reveal the predictive nature of the second measurement in (7), we first consider the difference

$$F_n = \mathfrak{m}_{n+1} \left( \frac{g}{\beta} \right) - \mathfrak{m}_n \left( \frac{T^*(\beta)g}{\beta} \right). \tag{9}$$

In the ideal case, utilizing (4) we get

$$\begin{split} F_n &= \mathfrak{m}_{n+1} \left( \frac{g}{\beta} \right) - \mathfrak{m}_n \left( \frac{T^*(\beta)g}{\beta} \right) \\ &= \left\langle T((n+1)\beta)u_0, \frac{g}{\beta} \right\rangle + \sum_{\tau_i < (n+1)\beta} \int_{\tau_i}^{(n+1)\beta} \left\langle T((n+1)\beta - s) f_i e^{\rho(\tau_i - s)}, \frac{g}{\beta} \right\rangle ds \\ &- \left\langle T(n\beta)u_0, \frac{T^*(\beta)g}{\beta} \right\rangle - \sum_{\tau_i < n\beta} \int_{\tau_i}^{n\beta} \left\langle T(n\beta - s) f_i e^{\rho(\tau_i - s)}, \frac{T^*(\beta)g}{\beta} \right\rangle ds \\ &= \int_{\tau_n}^{(n+1)\beta} \left\langle T((n+1)\beta - s) f_n e^{d(\tau_n - s)}, \frac{g}{\beta} \right\rangle ds \\ &+ \sum_{\tau_i < n\beta} \int_{\tau_i}^{(n+1)\beta} \left\langle T((n+1)\beta - s) f_i e^{\rho(\tau_i - s)}, \frac{g}{\beta} \right\rangle ds \\ &- \sum_{\tau_i < n\beta} \int_{\tau_i}^{n\beta} \left\langle T((n+1)\beta - s) f_n e^{\rho(\tau_n - s)}, \frac{g}{\beta} \right\rangle ds \\ &= \int_{\tau_n}^{(n+1)\beta} \left\langle T((n+1)\beta - s) f_n e^{\rho(\tau_n - s)}, \frac{g}{\beta} \right\rangle ds \\ &+ \sum_{\tau_i < n\beta} \int_{n\beta}^{(n+1)\beta} \left\langle T((n+1)\beta - s) f_i e^{\rho(\tau_i - s)}, \frac{g}{\beta} \right\rangle ds \end{split}$$

$$= \int_{\tau_n}^{(n+1)\beta} \left\langle T((n+1)\beta - s) f_n e^{\rho(\tau_n - s)}, \frac{g}{\beta} \right\rangle ds$$
$$+ \sum_{\tau_i < n\beta} e^{-\rho n\beta} \int_0^\beta \left\langle T(\beta - s) f_i e^{\rho(\tau_i - s)}, \frac{g}{\beta} \right\rangle ds.$$

**Remark 3.1** In the expression for  $F_n$  above, if no burst occurred in  $[n\beta, (n+1)\beta)$  (i.e.  $f_n=0$ ), then  $\int_{\tau_n}^{(n+1)\beta} \langle T((n+1)\beta-s)f_n e^{\rho(\tau_n-s)}, \frac{g}{\beta} \rangle ds=0$ . In addition, the term  $\sum_{\tau_i < n\beta} e^{-\rho n\beta} \int_0^\beta \langle T(\beta-s)f_i e^{\rho(\tau_i-s)}, \frac{g}{\beta} \rangle ds$  represents the effect of the bursts that had occurred before  $n\beta$ .

Secondly, we calculate the difference  $\Delta_n = e^{\rho\beta} F_{n+1} - F_n$ , which involves the measurements in two consecutive intervals  $[n\beta, (n+1)\beta)$  and  $[(n+1)\beta, (n+2)\beta)$ :

$$\begin{split} &\Delta_{n} = e^{\rho\beta} F_{n+1} - F_{n} \\ &= e^{\rho\beta} \int_{\tau_{n+1}}^{(n+2)\beta} \left\langle T((n+2)\beta - s) f_{n+1} e^{\rho(\tau_{n+1} - s)}, \frac{g}{\beta} \right\rangle ds \\ &+ \sum_{\tau_{i} < (n+1)\beta} e^{-\rho n\beta} \int_{0}^{\beta} \left\langle T(\beta - s) f_{i} e^{\rho(\tau_{i} - s)}, \frac{g}{\beta} \right\rangle ds \\ &- \int_{\tau_{n}}^{(n+1)\beta} \left\langle T((n+1)\beta - s) f_{n} e^{\rho(\tau_{n} - s)}, \frac{g}{\beta} \right\rangle ds \\ &- \sum_{\tau_{i} < n\beta} e^{-\rho n\beta} \int_{0}^{\beta} \left\langle T(\beta - s) f_{i} e^{\rho(\tau_{i} - s)}, \frac{g}{\beta} \right\rangle ds \\ &= e^{\rho\beta} \int_{\tau_{n+1}}^{(n+2)\beta} \left\langle T((n+2)\beta - s) f_{n+1} e^{\rho(\tau_{n+1} - s)}, \frac{g}{\beta} \right\rangle ds \\ &- \int_{\tau_{n}}^{(n+1)\beta} \left\langle T((n+1)\beta - s) f_{n} e^{\rho(\tau_{n} - s)}, \frac{g}{\beta} \right\rangle ds \\ &+ e^{-\rho n\beta} \int_{0}^{\beta} \left\langle T(\beta - s) f_{n} e^{\rho(\tau_{n} - s)}, \frac{g}{\beta} \right\rangle ds \\ &= e^{\rho\beta} \int_{\tau_{n+1}}^{(n+2)\beta} \left\langle T((n+2)\beta - s) f_{n+1} e^{\rho(\tau_{n+1} - s)}, \frac{g}{\beta} \right\rangle ds \\ &+ \int_{n\beta}^{\tau_{n}} \left\langle T((n+1)\beta - s) f_{n} e^{\rho(\tau_{n} - s)}, \frac{g}{\beta} \right\rangle ds . \end{split}$$

The above calculation leads us to the key observation

$$\Delta_n = 0$$
 in the ideal case if no burst occurred in  $[n\beta, (n+2)\beta)$ . (10)

In case the *j*-th burst did occur in the interval  $[(n+1)\beta, (n+2)\beta)$ , we use the following calculation to estimate the inner products  $\langle h_j, g \rangle$ . In view of Assumption 5, we have

🔊 Birkhäuser

15 Page 8 of 24 A. Aldroubi et al.

 $f_{n-1} = f_n = f_{n+2} = 0$  and, for  $\beta$  sufficiently small, we get

$$\begin{split} e^{3\rho\beta} F_{n+2} - F_{n-1} \\ &= e^{3\rho\beta} \int_{\tau_{n+2}}^{(n+3)\beta} \left\langle T((n+3)\beta - s) f_{n+2} e^{\rho(\tau_{n+2} - s)}, \frac{g}{\beta} \right\rangle ds \\ &+ \sum_{\tau_i < (n+2)\beta} e^{-\rho(n-1)\beta} \int_0^\beta \left\langle T(\beta - s) f_i e^{\rho(\tau_i - s)}, \frac{g}{\beta} \right\rangle ds \\ &- \int_{\tau_{n-1}}^{n\beta} \left\langle T(n\beta - s) f_{n-1} e^{\rho(\tau_{n-1} - s)}, \frac{g}{\beta} \right\rangle ds \\ &- \sum_{\tau_i < (n-1)\beta} e^{-\rho(n-1)\beta} \int_0^\beta \left\langle T(\beta - s) f_i e^{\rho(\tau_i - s)}, \frac{g}{\beta} \right\rangle ds \\ &= \int_0^\beta \left\langle T(\beta - s) f_{n+1} e^{\rho(\tau_{n+1} - (n-1)\beta - s)}, \frac{g}{\beta} \right\rangle ds \\ &= \int_0^\beta \left\langle T(\beta - s) f_j e^{\rho(t_j - (n-1)\beta - s)}, \frac{g}{\beta} \right\rangle ds \approx \langle h_j, g \rangle, \end{split}$$

where the last assertion is (essentially) yielded by the following lemma.

**Lemma 3.2** Assume that  $t_i \in [(n+1)\beta, (n+2)\beta)$  and

$$v_k(h_j, g, \beta) = \left| \int_0^\beta \left\langle T(\beta - s) h_j e^{\rho(t_j - (n - k)\beta - s)}, \frac{g}{\beta} \right\rangle ds - \langle h_j, g \rangle \right|, \ k = 0, 1.$$
(11)

Then

$$v_k(h_j, g, \beta) \le \|g\| \left( M \|h_j\| (e^{(k+2)\rho\beta} - 1) \mathbf{e}(a\beta) + \sup_{s \in [0, \beta]} \|T(s)h_j - h_j\| \right), \tag{12}$$

where M and a are as in Proposition 2.2 and

$$\mathbf{e}(t) = \begin{cases} \frac{e^t - 1}{t}, & t \neq 0; \\ 1, & t = 0. \end{cases}$$
 (13)

In particular,  $v_k(h_j, g, \beta) \to 0$  as  $\beta \to 0$ .

**Proof** Observe that

$$v_k(h_j, g, \beta) = \left| \int_0^\beta \left\langle T(\beta - s) h_j e^{\rho(t_j - (n - k)\beta - s)}, \frac{g}{\beta} \right\rangle ds - \langle h_j, g \rangle \right|$$

Birkhäuser 🖹

Content courtesy of Springer Nature, terms of use apply. Rights reserved.

$$= \left| \int_{0}^{\beta} \left\langle T(\beta - s)h_{j}e^{\rho(t_{j} - (n-k)\beta - s)} - h_{j}, \frac{g}{\beta} \right\rangle ds \right|$$

$$\leq \int_{0}^{\beta} \|T(\beta - s)h_{j}e^{\rho(t_{j} - (n-k)\beta - s)} - h_{j}\| \frac{\|g\|}{\beta} ds$$

$$\leq \frac{\|g\|}{\beta} \int_{0}^{\beta} \|T(\beta - s)h_{j}e^{\rho(t_{j} - (n-k)\beta - s)} - T(\beta - s)h_{j}\| ds$$

$$+ \frac{\|g\|}{\beta} \int_{0}^{\beta} \|T(\beta - s)h_{j} - h_{j}\| ds$$

$$= I_{1} + I_{2}. \tag{14}$$

Using Proposition 2.2, i.e. the inequality  $||T(t)|| \le Me^{at}$ , we get

$$I_{1} = \frac{\|g\|}{\beta} \int_{0}^{\beta} \|T(\beta - s)h_{j}e^{\rho(t_{j} - (n - k)\beta - s)} - T(\beta - s)h_{j}\|ds$$

$$\leq \frac{\|g\|}{\beta} \int_{0}^{\beta} \|T(\beta - s)\|\|h_{j}\|(e^{(k+2)\rho\beta} - 1)ds$$

$$\leq \|g\|M\|h_{j}\|(e^{(k+2)\rho\beta} - 1)\frac{1}{\beta} \int_{0}^{\beta} e^{a(\beta - s)}ds$$

$$\leq \|g\|\|h_{j}\|M(e^{(k+2)\rho\beta} - 1)\mathbf{e}(a\beta)$$
(15)

and

$$I_{2} = \frac{\|g\|}{\beta} \int_{0}^{\beta} \|T(\beta - s)h_{j} - h_{j}\|ds$$

$$= \frac{\|g\|}{\beta} \int_{0}^{\beta} \|T(s)h_{j} - h_{j}\|ds$$

$$\leq \|g\| \sup_{s \in [0,\beta]} \|T(s)h_{j} - h_{j}\|. \tag{16}$$

Estimate (12) immediately follows from (14), (15), and (16). We get  $\lim_{\beta \to 0} v_k(h_j, g, \beta) = 0$  since  $\lim_{\beta \to 0} (e^{(k+2)\rho\beta} - 1)\mathbf{e}(a\beta) = 0$  and  $\lim_{\beta \to 0} \sup_{s \in [0,\beta]} ||T(s)h_j - h_j|| = 0$  due to the strong continuity of the semigroup T.  $\square$ 

Equipped with the above observations, we are naturally led to Algorithm 1 below. The algorithm turns out to be robust both with respect to the considered additive measurement noise and introduction of a background source as described in the following Theorem 3.3.

🔊 Birkhäuser

15 Page 10 of 24 A. Aldroubi et al.

**Algorithm 1.** Pseudo-code for approximating the time and shape of a possible burst with prescribed exponential decay

```
Input: Measurements: \mathfrak{m}_n(\frac{g}{\beta}), \mathfrak{m}_n(\frac{T^*(\beta)g}{\beta}) and threshold: Q(g,\beta), g \in \widetilde{G}
  1:
         Compute F_i = \mathfrak{m}_{i+1}(\frac{g}{\beta}) - \mathfrak{m}_i(\frac{T^*(\beta)g}{\beta})
 2:
         Compute e^{\rho\beta}F_{i+1} - F_i
  3:
         For g \in \widetilde{G} do
 4:
            i=1
 5:
 6:
            while i\beta < T
                if e^{\rho\beta}F_{i+1} - F_i > Q(g,\beta) then
 7:
                   f(g) := e^{3\rho\beta} F_{i+2} - F_{i-1}
 8:
 9:
                   \mathfrak{t} := (i+1)\beta
                   i = i + 3
10:
                else
11:
                   if e^{\rho\beta}F_{i+2}-F_{i+1}>Q(g,\beta) then
12:
                      f(g) := e^{3\rho\beta} F_{i+3} - F_i
13:
                      \mathfrak{t} := (i+2)\beta
14:
15:
                      i = i + 3
16:
                   else
                      i = i + 1
17:
         Output: \mathfrak{t} and \mathfrak{f}(g) for all g \in \widetilde{G}.
18:
```

**Theorem 3.3** *Under Assumptions* 1, 3, 4 and 5, and M, a as in Proposition 2.2, let

$$Q(g,\beta) = e^{(\rho+a)\beta} M L \|g\|\beta + e^{a\beta} (e^{\beta} - 1) M K \|g\| + 4e^{\rho\beta} \sigma$$
 (17)

be the threshold in Algorithm 1. Let also  $\mathfrak{t}_j$  and  $\mathfrak{f}_j(g)$  be the outputs of Algorithm 1. Then  $|\mathfrak{t}_j - t_j| \leq \beta$  and

$$|f_{j}(g) - \langle h_{j}, g \rangle|$$

$$\leq 3e^{(3\rho + a)\beta} ML ||g||\beta + e^{a\beta} (e^{3\rho\beta} - 1) MK ||g|| + 4e^{3\rho\beta} \sigma$$

$$+2e^{\rho\beta} Q(g, \beta) + \max\{v_{0}(h_{j}, g, \beta), v_{1}(h_{j}, g, \beta)\},$$
(18)

where  $v_k$ , k = 0, 1, are given by (12). In particular, for sufficiently small  $\beta > 0$ , one has  $|f_j(g) - \langle h_j, g \rangle| \le 13\sigma$  as long as  $\sigma > 0$ .

**Proof** Adjusting the computations in the ideal case to account for the noise and the background source, we get

$$F_{n} = \mathfrak{m}_{n+1} \left( \frac{g}{\beta} \right) - \mathfrak{m}_{n} \left( \frac{T^{*}(\beta)g}{\beta} \right)$$

$$= \int_{\tau_{n}}^{(n+1)\beta} \left\langle T((n+1)\beta - s) f_{n} e^{\rho(\tau_{n} - s)}, \frac{g}{\beta} \right\rangle ds$$

$$+ \sum_{\tau_{i} < n\beta} \int_{0}^{\beta} \left\langle T(\beta - s) f_{i} e^{\rho(\tau_{i} - n\beta - s)}, \frac{g}{\beta} \right\rangle ds$$

$$+ \int_{0}^{\beta} \left\langle T(\beta - s) \eta(n\beta + s), \frac{g}{\beta} \right\rangle ds + \nu \left( (n+1)\beta, \frac{g}{\beta} \right) - \nu \left( n\beta, \frac{T^{*}(\beta)g}{\beta} \right).$$

The difference  $\Delta_n = e^{\rho\beta} F_{n+1} - F_n$  not only allows us to detect the burst in the ideal case (where it kills the effect of the past bursts according to (10)), but also, as we shall see presently, mitigates the effect of the background source. Once again, adjusting the previous computations for noise and background source, we get

$$\begin{split} \Delta_n &= e^{\rho\beta} F_{n+1} - F_n \\ &= \int_{\tau_{n+1}}^{(n+2)\beta} \left\langle T((n+2)\beta - s) f_{n+1} e^{\rho(\tau_{n+1} + \beta - s)}, \frac{g}{\beta} \right\rangle ds \\ &+ \int_{n\beta}^{\tau_n} \left\langle T((n+1)\beta - s) f_n e^{\rho(\tau_n - s)}, \frac{g}{\beta} \right\rangle ds \\ &+ e^{\rho\beta} \int_0^\beta \left\langle T(\beta - s) \eta((n+1)\beta + s), \frac{g}{\beta} \right\rangle ds \\ &- \int_0^\beta \left\langle T(\beta - s) \eta(n\beta + s), \frac{g}{\beta} \right\rangle ds + \alpha_n, \end{split}$$

where  $\alpha_n = e^{\rho\beta}v\Big((n+2)\beta, \frac{g}{\beta}\Big) - e^{\rho\beta}v\Big((n+1)\beta, \frac{T^*(\beta)g}{\beta}\Big) - v\Big((n+1)\beta, \frac{g}{\beta}\Big) + v\Big(n\beta, \frac{T^*(\beta)g}{\beta}\Big).$ 

 $v\left(n\beta,\frac{T^*(\beta)g}{\beta}\right)$ . We remark that Assumption 5  $(t_{j+1}-t_j>4\beta)$  implies that, at most one of the terms  $f_n,\,f_{n+1}$  is non-zero in the expression of  $e^{\rho\beta}F_{n+1}-F_n$  above.

Firstly, we prove that if no burst occurred in  $[n\beta, (n+2)\beta)$  (i.e.  $f_n = f_{n+1} = 0$ ), then  $|\Delta_n|$  is below our chosen threshold (17). The proof is achieved via the following computations that make use of Assumptions 3 and 4:

$$\begin{aligned} |\Delta_n| &= \left| e^{\rho\beta} F_{n+1} - F_n \right| \\ &= \left| e^{\rho\beta} \int_0^\beta \left\langle T(\beta - s) \eta((n+1)\beta + s), \frac{g}{\beta} \right\rangle ds - \int_0^\beta \left\langle T(\beta - s) \eta(n\beta + s), \frac{g}{\beta} \right\rangle ds + \alpha_n \right| \\ &\leq \left| e^{\rho\beta} \int_0^\beta \left\langle T(\beta - s) \eta((n+1)\beta + s), \frac{g}{\beta} \right\rangle ds - e^{\rho\beta} \int_0^\beta \left\langle T(\beta - s) \eta(n\beta + s), \frac{g}{\beta} \right\rangle ds \right| \end{aligned}$$

15 Page 12 of 24 A. Aldroubi et al.

$$+\left|e^{\rho\beta}\int_{0}^{\beta}\left\langle T(\beta-s)\eta(n\beta+s),\frac{g}{\beta}\right\rangle ds - \int_{0}^{\beta}\left\langle T(\beta-s)\eta(n\beta+s),\frac{g}{\beta}\right\rangle ds\right| + |\alpha_{n}|$$

$$\leq e^{\rho\beta}\int_{0}^{\beta}\|\eta((n+1)\beta+s) - \eta(n\beta+s)\|\|T^{*}(\beta-s)\frac{g}{\beta}\|ds$$

$$+(e^{\rho\beta}-1)\int_{0}^{\beta}\|\eta(n\beta+s)\|\|T^{*}(\beta-s)\frac{g}{\beta}\|ds + 4e^{\rho\beta}\sigma$$

$$\leq e^{\rho\beta}CL\|g\|\beta + (e^{\rho\beta}-1)CK\|g\| + 4e^{\rho\beta}\sigma = Q(g,\beta)$$

$$(19)$$

where  $C = Me^{a\beta}$  so that  $||T^*(\beta - s)|| \le C$ .

Secondly, assume that the *j*-th burst with the shape  $h_j$  occurred in the interval  $[(n+1)\beta, (n+2)\beta)$ . To analyze this situation, we will look at two cases: (1) the *j*-th burst is detected by our algorithm; and (2) the *j*-th burst is not detected. For Case 1, the burst is detected if and only if  $|\Delta_n| > Q(g, \beta)$  or  $|\Delta_{n+1}| > Q(g, \beta)$  and we need to prove (18). For Case 2, when the *j*-th burst is not detected, we will show that  $\langle h_j, g \rangle$  is small, i.e. (18) holds with  $f_j(g) = 0$ .

Case 1. The j-th burst is detected in  $[(n+1)\beta, (n+2)\beta)$ .

Assume that  $|\Delta_n| > Q(g, \beta)$ . Then  $\tau_{n+1} = t_j$ ,  $f_{n+1} = h_j$ ,  $f_{n-1} = f_n = f_{n+2} = 0$  and Algorithm 1 returns  $\mathfrak{t}_j = (n+1)\beta$  and  $\mathfrak{f}_j(g) = e^{3\rho\beta}F_{n+2} - F_{n-1}$ . We need to establish (18), i.e. show that  $\langle h_j, g \rangle \approx e^{3\rho\beta}F_{n+2} - F_{n-1}$  for small  $\beta$ . We get

$$e^{3\rho\beta} F_{n+2} - F_{n-1}$$

$$= \int_0^\beta \left\langle T(\beta - s)h_j e^{\rho(t_j - (n-1)\beta - s)}, \frac{g}{\beta} \right\rangle ds$$

$$+ e^{3\rho\beta} \int_0^\beta \left\langle T(\beta - s)\eta((n+2)\beta + s), \frac{g}{\beta} \right\rangle ds$$

$$- \int_0^\beta \left\langle T(\beta - s)\eta((n-1)\beta + s), \frac{g}{\beta} \right\rangle ds + \alpha'_{n-1}$$

where  $\alpha'_{n-1} = e^{3\rho\beta}v\Big((n+3)\beta,\frac{g}{\beta}\Big) - e^{3\rho\beta}v\Big((n+2)\beta,\frac{T^*(\beta)g}{\beta}\Big) - v\Big(n\beta,\frac{g}{\beta}\Big) + v\Big((n-1)\beta,\frac{T^*(\beta)g}{\beta}\Big)$ . Therefore,

$$\begin{aligned} &\left| \mathsf{f}_{j}(g) - \langle h_{j}, g \rangle \right| \\ &= |e^{3\rho\beta} F_{n+2} - F_{n-1} - \langle h_{j}, g \rangle | \\ &\leq \left| \int_{0}^{\beta} \left\langle T(\beta - s) h_{j} e^{\rho(t_{j} - (n-1)\beta - s)}, \frac{g}{\beta} \right\rangle ds - \langle h_{j}, g \rangle \right| + 4e^{3\rho\beta} \sigma \\ &+ \left| e^{3\rho\beta} \int_{0}^{\beta} \left\langle T(\beta - s) \eta((n+2)\beta + s), \frac{g}{\beta} \right\rangle ds \\ &- \int_{0}^{\beta} \left\langle T(\beta - s) \eta((n-1)\beta + s), \frac{g}{\beta} \right\rangle ds \right| \\ &\leq v_{1}(h_{j}, g, \beta) + 3e^{3\rho\beta} CL \|g\|\beta + (e^{3\rho\beta} - 1)CK \|g\| + 4e^{3\rho\beta} \sigma. \end{aligned}$$

where  $C = Me^{a\beta}$  and  $v_1(h_j, g, \beta)$  is given by (12). Thus, estimate (18) is established for the case when  $|\Delta_n| > Q(g, \beta)$ .

Assume now that  $|\Delta_n| \le Q(g, \beta)$  and  $|\Delta_{n+1}| > Q(g, \beta)$ . In this case, Algorithm 1 returns  $\mathfrak{t}_j = (n+2)\beta$  and  $\mathfrak{f}_j(g) = e^{3\rho\beta}F_{n+3} - F_n$ . In particular,

$$\begin{aligned} |\mathfrak{f}_{j}(g) - \langle h_{j}, g \rangle| \\ &\leq \left| \int_{0}^{\beta} \left\langle T(\beta - s) h_{j} e^{\rho(t_{j} - n\beta - s)}, \frac{g}{\beta} \right\rangle ds - \langle h_{j}, g \rangle \right| \\ &+ 3e^{3\rho\beta} CL \|g\|\beta + (e^{3\rho\beta} - 1)CK \|g\| + 4e^{3\rho\beta} \sigma, \end{aligned}$$

where  $|\int_0^\beta \left\langle T(\beta-s)h_j e^{\rho(t_j-n\beta-s)}, \frac{g}{\beta} \right\rangle ds - \langle h_j, g \rangle| = v_0(h_j, g, \beta)$  is given by (12). Thus, estimate (18) holds when  $|\Delta_{n+1}| > Q(g, \beta)$  as well, and Case 1 is covered.

Case 2. The j-th burst is in  $[(n+1)\beta, (n+2)\beta)$ , but  $\langle h_j, g \rangle$  is too small to be detected. We need to show that (18) holds with  $\mathfrak{f}_j(g) = 0$ . We have

$$e^{2\rho\beta}F_{n+2} - F_n$$

$$= \int_0^\beta \left\langle T(\beta - s)h_j e^{\rho(t_j - n\beta - s)}, \frac{g}{\beta} \right\rangle ds + e^{2\rho\beta} \int_0^\beta \left\langle T(\beta - s)\eta((n+2)\beta + s), \frac{g}{\beta} \right\rangle ds$$

$$- \int_0^\beta \left\langle T(\beta - s)\eta(n\beta + s), \frac{g}{\beta} \right\rangle ds + \alpha_n''$$
(20)

where  $\alpha_n'' = e^{2\rho\beta}v\Big((n+3)\beta,\frac{g}{\beta}\Big) - e^{2\rho\beta}v\Big((n+2)\beta,\frac{T^*(\beta)g}{\beta}\Big) - v\Big((n+1)\beta,\frac{g}{\beta}\Big) + v\Big(n\beta,\frac{T^*(\beta)g}{\beta}\Big)$ . Using (20) to estimate  $\langle h_j,g\rangle$ , we get

$$\begin{aligned} \left| \langle h_{j}, g \rangle \right| \\ &\leq \left| -\int_{0}^{\beta} \left\langle T(\beta - s)h_{j}e^{\rho(t_{j} - n\beta - s)}, \frac{g}{\beta} \right\rangle ds \right| \\ &+ \left| \int_{0}^{\beta} \left\langle T(\beta - s)h_{j}e^{\rho(t_{j} - n\beta - s)}, \frac{g}{\beta} \right\rangle ds - \langle h_{j}, g \rangle \right| \\ &\leq \left| -\int_{0}^{\beta} \left\langle T(\beta - s)h_{j}e^{\rho(t_{j} - n\beta - s)}, \frac{g}{\beta} \right\rangle ds + (e^{2\rho\beta}F_{n+2} - F_{n}) \right| \\ &+ \left| F_{n} - e^{2\rho\beta}F_{n+2} \right| + v_{0}(h_{j}, g, \beta) \\ &\leq \left| e^{2\rho\beta} \int_{0}^{\beta} \left\langle T(\beta - s)\eta((n+2)\beta + s), \frac{g}{\beta} \right\rangle ds \\ &- \int_{0}^{\beta} \left\langle T(\beta - s)\eta(n\beta + s), \frac{g}{\beta} \right\rangle ds + \alpha_{n}'' \right| \\ &+ e^{\rho\beta} \left| e^{\rho\beta}F_{n+2} - F_{n+1} \right| + \left| e^{\rho\beta}F_{n+1} - F_{n} \right| + v_{0}(h_{j}, g, \beta) \\ &\leq 2e^{2\rho\beta}CL\|g\|\beta + (e^{2\rho\beta} - 1)CK\|g\| + 4e^{2\rho\beta}\sigma + 2e^{\rho\beta}O(g, \beta) + v_{0}(h_{j}, g, \beta), \end{aligned}$$

🕅 Birkhäuser

15 Page 14 of 24 A. Aldroubi et al.

where we have used the fact that  $\left|e^{\rho\beta}F_{n+2} - F_{n+1}\right| \leq Q(g,\beta), \left|e^{\rho\beta}F_{n+1} - F_n\right| \leq Q(g,\beta)$ , and estimated the term  $\left|e^{2\rho\beta}\int_0^\beta \left\langle T(\beta-s)\eta((n+2)\beta+s), \frac{g}{\beta}\right\rangle ds - \int_0^\beta \left\langle T(\beta-s)\eta(n\beta+s), \frac{g}{\beta}\right\rangle ds + \alpha_n''$  in a similar way as (19). The above estimates establish (18) in Case 2, and the theorem is proved.

## 3.2 Model with general decay function

In this section, we consider the same dynamical system, but we discuss a more general situation. Here the decay function  $\phi$  does not have a concrete formula, but its decay velocity is restricted. The model is as follows:

$$\begin{cases} \dot{u}(t) = Au(t) + \sum_{j=1}^{N} h_{j} \phi(t - t_{j}) \chi_{[t_{j}, \infty)}(t) + \eta, \\ u(0) = u_{0}, \end{cases}$$
 (21)

where the function  $\phi$  is continuous on  $[0, \infty)$  and satisfies  $\phi(0) = 1$  and

$$0 < \phi(t) \le e^{-\rho t} \tag{22}$$

for some  $\rho > 0$ .

In this model, we continue to use the constants introduced in Proposition 2.2 and Assumptions 1 to 5, as well as  $C = Me^{a\beta}$ . We also assume that the bursts are uniformly bounded as mentioned in Assumption 2. The constant D in Assumption 5 that controls the time gap between the bursts  $(t_{j+1} - t_j \ge D + 4\beta)$  is chosen in a way that

$$\epsilon = \frac{2}{\rho^D - 1} CHR \tag{23}$$

is a small quantity. We shall also need the following modification of the technical Lemma 3.2.

**Lemma 3.4** Assume that  $t_i \in [(n+1)\beta, (n+2)\beta)$  and

$$v_{k,i}(h_j, g, \beta) = \left| \int_0^\beta \left\langle T(\beta - s)h_j e^{k\rho\beta} \phi((n+i)\beta + s - t_j), \frac{g}{\beta} \right\rangle ds - \left\langle h_j, g \right\rangle \right|, \ k, i = 2, 3.$$
(24)

Then

$$v_{k,i}(h_j, g, \beta) \le \|g\| \left( \|h_j\| M \max_{s \in [(i-2)\beta, i\beta]} |e^{k\rho\beta} \phi(s) - 1| \mathbf{e}(a\beta) + \sup_{s \in [0,\beta]} \|T(s)h_j - h_j\| \right), \tag{25}$$

Birkhäuser 🖹

Content courtesy of Springer Nature, terms of use apply. Rights reserved.

where **e** is given by (13). In particular,  $v_{k,i}(h_j, g, \beta) \to 0$  as  $\beta \to 0$ , k, i = 2, 3. **Proof** Similarly to (14), we separate each  $v_{k,i}(h_i, g, \beta)$ , k, i = 2, 3, into two parts:

$$\left| \int_{0}^{\beta} \left\langle T(\beta - s)h_{j}e^{k\rho\beta}\phi((n+i)\beta + s - t_{j}), \frac{g}{\beta} \right\rangle ds - \langle h_{j}, g \rangle \right|$$

$$\leq \frac{\|g\|}{\beta} \int_{0}^{\beta} \|T(\beta - s)h_{j}e^{k\rho\beta}\phi((n+i)\beta + s - t_{j}) - T(\beta - s)h_{j}\|ds$$

$$+ \frac{\|g\|}{\beta} \int_{0}^{\beta} \|T(\beta - s)h_{j} - h_{j}\|ds$$

$$= I_{1} + I_{2}.$$

Estimate for  $I_2$  is still given by (16). For  $I_1$ , by  $||T(t)|| \le Me^{at}$ , we have

$$\begin{split} I_1 &= \frac{\|g\|}{\beta} \int_0^\beta \|T(\beta - s)h_j e^{k\rho\beta} \phi((n+i)\beta + s - t_j) - T(\beta - s)h_j \|ds \\ &\leq \frac{\|g\|}{\beta} \int_0^\beta \|T(\beta - s)\| \|h_j\| |e^{k\rho\beta} \phi((n+i)\beta + s - t_j) - 1| ds \\ &= \|g\| \|h_j\| M \max_{s \in [(i-2)\beta, i\beta]} |e^{k\rho\beta} \phi(s) - 1| \mathbf{e}(a\beta). \end{split}$$

By the assumption on  $\phi$ ,  $I_1 \to 0$  as  $\beta \to 0$ .

**Algorithm 2** Pseudo-code for approximating the time and shape of a possible burst with varying decay

```
Input: Measurements: \mathfrak{m}_n(\frac{g}{\beta}), \mathfrak{m}_n(\frac{T^*(\beta)g}{\beta}); threshold: Q_1(g,\beta),
          for g \in \widetilde{G}; a parameter D > 0
          Compute F_i = \mathfrak{m}_{i+1}(\frac{g}{\beta}) - \mathfrak{m}_i(\frac{T^*(\beta)g}{\beta})
          Compute e^{\rho\beta}F_{i+1} - F_i
  4:
          For g \in \widetilde{G} do
  5:
          i=1
              while i\beta < T do
  6:
                  if e^{\rho\beta}F_{i+1} - F_i > Q_1(g,\beta) then
  7:
                     f(g) := e^{3\rho\beta} F_{i+2} - F_{i-1}
                     \mathfrak{t} := (i+1)\beta
  9:
                     i = i + 3 + \lfloor \frac{D}{R} \rfloor
10:
11:
                     if e^{\rho\beta}F_{i+2} - F_{i+1} > Q_1(g, \beta) then f(g) := e^{3\rho\beta}F_{i+3} - F_i
12:
13:
                         \mathfrak{t} := (i+2)\beta
14:
                        i = i + 3 + \lfloor \frac{D}{R} \rfloor
15:
16:
17:
                        i = i + 1
           Output: \mathfrak{t} and \mathfrak{f}(g) for all g \in \widetilde{G}.
18:
```

15 Page 16 of 24 A. Aldroubi et al.

**Theorem 3.5** *Under Assumptions* 1 to 5,  $Q(g, \beta)$  given by (17), and  $\epsilon$ —by (23), let

$$Q_1(g,\beta) = Q(g,\beta) + \epsilon \tag{26}$$

be the threshold in Algorithm 2. Let also  $\mathfrak{t}_j$  and  $\mathfrak{f}_j(g)$  be the outputs of Algorithm 2. Then  $|\mathfrak{t}_j - t_j| \leq \beta$  and

$$|f_{j}(g) - \langle h_{j}, g \rangle|$$

$$\leq \epsilon + 3e^{(3\rho + a)\beta} ML ||g||\beta + e^{a\beta} (e^{3\rho\beta} - 1) MK ||g|| + 4e^{3\rho\beta} \sigma$$

$$+ 2e^{\rho\beta} Q_{1}(g, \beta) + \max\{v_{3,2}(h_{j}, g, \beta), v_{3,3}(h_{j}, g, \beta), v_{2,2}(h_{j}, g, \beta)\}$$
 (27)

where  $v_{k,i}$ , k, i=2,3, are defined by (24) so that  $v_{k,i}(h_j,g,\beta) \to 0$  as  $\beta \to 0$  (by Lemma 3.4). In particular, for sufficiently small  $\beta > 0$ , one has  $|f_j(g) - \langle h_j, g \rangle| \le 13\sigma + 4\epsilon$  as long as  $\sigma$  and  $\epsilon$  are not both 0.

**Proof** Suppose that we have detected the (j-1)-th burst in the time interval  $[m\beta, (m+2)\beta)$  for some  $m \in \mathbb{N}$ . By Assumption 5, the next nonzero burst  $h_j$  must happen no sooner than  $m\beta + D + 4\beta$ , thus we just need to continue our detection from  $(m+3+\lfloor\frac{D}{\beta}\rfloor)\beta$ . Now we simply denote  $(m+3+\lfloor\frac{D}{\beta}\rfloor)$  by n and analyze the occurrence of a burst in the interval  $[n\beta, (n+2)\beta)$ . To do that, we first evaluate the quantities  $F_n$  and  $\Delta_n = e^{\rho\beta}F_{n+1} - F_n$  from the measurements (7):

$$\begin{split} F_n &= \mathfrak{m}_{n+1} \left( \frac{g}{\beta} \right) - \mathfrak{m}_n \left( \frac{T^*(\beta)g}{\beta} \right) \\ &= \int_{\tau_n}^{(n+1)\beta} \left\langle T((n+1)\beta - s) f_n \phi(s - \tau_n), \frac{g}{\beta} \right\rangle ds \\ &+ \sum_{\tau_i < n\beta} \int_0^\beta \left\langle T(\beta - s) f_i \phi(n\beta + s - \tau_i), \frac{g}{\beta} \right\rangle ds \\ &+ \int_0^\beta \left\langle T(\beta - s) \eta(n\beta + s), \frac{g}{\beta} \right\rangle ds + \nu \left( (n+1)\beta, \frac{g}{\beta} \right) - \nu \left( n\beta, \frac{T^*(\beta)g}{\beta} \right), \end{split}$$

and

$$\begin{split} &\Delta_n = e^{\rho\beta} \, f_{n+1} - F_n \\ &= e^{\rho\beta} \int_{\tau_{n+1}}^{(n+2)\beta} \left\langle T((n+2)\beta - s) \, f_{n+1} \phi(s - \tau_{n+1}), \frac{g}{\beta} \right\rangle ds \\ &+ \int_0^\beta \left\langle T(\beta - s) \, f_n e^{\rho\beta} \phi((n+1)\beta + s - \tau_n), \frac{g}{\beta} \right\rangle ds \\ &- \int_{\tau_n}^{(n+1)\beta} \left\langle T((n+1)\beta - s) \, f_n \phi(s - \tau_n), \frac{g}{\beta} \right\rangle ds \\ &+ \sum_{T \leq n\beta} \int_0^\beta \left\langle T(\beta - s) \, f_i(e^{\rho\beta} \phi((n+1)\beta + s - \tau_i) - \phi(n\beta + s - \tau_i)), \frac{g}{\beta} \right\rangle ds \end{split}$$

$$+e^{\rho\beta}\int_0^\beta \left\langle T(\beta-s)\eta((n+1)\beta+s),\frac{g}{\beta}\right\rangle ds - \int_0^\beta \left\langle T(\beta-s)\eta(n\beta+s),\frac{g}{\beta}\right\rangle ds + \alpha_n$$

where  $\alpha_n = e^{\rho\beta} v \left( (n+2)\beta, \frac{g}{\beta} \right) - e^{\rho\beta} v \left( (n+1)\beta, \frac{T^*(\beta)g}{\beta} \right) - v \left( (n+1)\beta, \frac{g}{\beta} \right) + v \left( n\beta, \frac{T^*(\beta)g}{\beta} \right)$ . From the expression above, we note that since we don't have a concrete formula for  $\phi(t)$ , we are unable to use the technique in Sect. 3.1 to cancel the effect of the bursts that occurred prior to  $n\beta$ . However, by Assumption 5, the requirement that the distance  $|t_{j+1} - t_j|$  between two bursts is large enough, ensures that if no burst occurred in  $[n\beta, (n+2)\beta)$  (i.e.  $f_n = f_{n+1} = 0$ ), then  $|e^{\rho\beta}F_{n+1} - F_n|$  is below our chosen threshold (26). We will show that via the calculations below, where we use (19), (22) and Assumption 5.

$$\begin{split} |\Delta_{n}| &= |e^{\rho\beta}F_{n+1} - F_{n}| \\ &\leq \sum_{\tau_{i} < n\beta} \left| \int_{0}^{\beta} \left\langle T(\beta - s) f_{i}(e^{\rho\beta}\phi((n+1)\beta + s - \tau_{i}) - \phi(n\beta + s - \tau_{i})), \frac{g}{\beta} \right\rangle ds \right| \\ &+ \left| \int_{0}^{\beta} \left\langle T(\beta - s)(e^{\rho\beta}\eta((n+1)\beta + s) - \eta(n\beta + s)), \frac{g}{\beta} \right\rangle ds \right| + |\alpha_{n}| \\ &\leq \sum_{\tau_{i} < n\beta} \int_{0}^{\beta} |e^{\rho\beta}\phi((n+1)\beta + s - \tau_{i}) - \phi(n\beta + s - \tau_{i})| \|f_{i}\| \|T^{*}(\beta - s)\frac{g}{\beta} \|ds + e^{\rho\beta}CL\|g\|\beta + (e^{\rho\beta} - 1)CK\|g\| + 4e^{\rho\beta}\sigma \\ &\leq \sum_{\tau_{i} < n\beta} 2e^{-\rho(n\beta - \tau_{i})}C\|f_{i}\|\|g\| + w(C, L, g, \beta, K, \sigma) \\ &= \sum_{k=1}^{j-1} 2e^{-\rho(n\beta - t_{k})}C\|h_{k}\|\|g\| + w(C, L, g, \beta, K, \sigma) \\ &\leq \sum_{k=1}^{\infty} 2e^{-k\rho D}CHR + w(C, L, g, \beta, K, \sigma) \\ &\leq \frac{2}{e^{\rho D} - 1}CHR + w(C, L, g, \beta, K, \sigma) \\ &\leq \epsilon + w(C, L, g, \beta, K, \sigma) = Q_{1}(g, \beta) \end{split}$$

where  $w(C,L,g,\beta,K,\sigma)=e^{\rho\beta}CL\|g\|\beta+(e^{\rho\beta}-1)CK\|g\|+4e^{\rho\beta}\sigma$ . Recall that in the above calculation  $C=Me^{a\beta},\ \epsilon=\frac{2}{e^{\rho D}-1}CHR$  as defined by (23), H is the upper bound constant in Assumption 2, L,K are the Lipschitz constant and the background source upper bound, respectively, in Assumption 3, and  $R=\sup_{g\in\widetilde{G}}\|g\|$  as in Assumption 1.

**Remark 3.6** In this case, the time difference D between every pair of adjacent non-zero bursts will influence the error estimate. When  $\epsilon < \sigma$ , the past bursts only have a very weak impact on the subsequent bursts and their influence together is even smaller than the noise level  $\sigma$ .

15 Page 18 of 24 A. Aldroubi et al.

We now assume that the *j*-th burst occurred in the interval  $[(n+1)\beta, (n+2)\beta)$ . Similarly to our discussion in Sect. 3.1, we consider two cases: (1) the burst is detected; and (2) the burst is not detected. As before, for Case 1, the burst is detected if and only if  $|\Delta_n| > Q_1(g, \beta)$  or  $|\Delta_{n+1}| > Q_1(g, \beta)$ . We need to establish (27) for each of the cases (assuming  $f_j(g) = 0$  in Case 2).

Case 1. The j-th burst is detected in  $[(n+1)\beta, (n+2)\beta)$ .

Assume that  $|\Delta_n| > Q_1(g,\beta)$ . Then  $\tau_{n+1} = t_j$ ,  $f_{n+1} = h_j$ ,  $f_{n-1} = f_n = f_{n+2} = 0$  and Algorithm 2 returns  $\mathfrak{t}_j = (n+1)\beta$  and  $\mathfrak{f}_j(g) = e^{3\rho\beta}F_{n+2} - F_{n-1}$ . We get

$$\begin{split} e^{3\rho\beta}F_{n+2} - F_{n-1} \\ &= \int_{0}^{\beta} \left\langle T(\beta - s)h_{j}e^{3\rho\beta}\phi((n+2)\beta + s - t_{j}), \frac{g}{\beta} \right\rangle ds \\ &+ \sum_{\tau_{i} < (n-1)\beta} \int_{0}^{\beta} \left\langle T(\beta - s)f_{i}(e^{3\rho\beta}\phi((n+2)\beta + s - \tau_{i}) - \phi((n-1)\beta + s - \tau_{i})), \frac{g}{\beta} \right\rangle ds \\ &+ e^{3\rho\beta} \int_{0}^{\beta} \left\langle T(\beta - s)\eta((n+2)\beta + s), \frac{g}{\beta} \right\rangle ds \\ &- \int_{0}^{\beta} \left\langle T(\beta - s)\eta((n-1)\beta + s), \frac{g}{\beta} \right\rangle ds + \alpha_{n-1}' \end{split}$$

where 
$$\alpha_{n-1}' = e^{3\rho\beta} v \left( (n+3)\beta, \frac{g}{\beta} \right) - e^{3\rho\beta} v \left( (n+2)\beta, \frac{T^*(\beta)g}{\beta} \right) - v \left( n\beta, \frac{g}{\beta} \right) + v \left( (n-1)\beta, \frac{T^*(\beta)g}{\beta} \right).$$

Computing the error gives

$$\begin{aligned} & |\mathfrak{f}_{j}(g) - \langle h_{j}, g \rangle | \\ &= |e^{3\rho\beta} F_{n+2} - F_{n-1} - \langle h_{j}, g \rangle | \\ &\leq \left| \int_{0}^{\beta} \left\langle T(\beta - s) h_{j} e^{3\rho\beta} \phi((n+2)\beta + s - t_{j}), \frac{g}{\beta} \right\rangle ds - \langle h_{j}, g \rangle \right| + \left| \alpha_{n-1}' \right| \\ &+ \left| \sum_{\tau_{i} < (n-1)\beta} \int_{0}^{\beta} \left\langle T(\beta - s) f_{i} (e^{3\rho\beta} \phi((n+2)\beta + s - \tau_{i}) - \phi((n-1)\beta + s - \tau_{i})), \frac{g}{\beta} \right\rangle ds \right| \\ &+ \left| \int_{0}^{\beta} \left\langle T(\beta - s) e^{3\rho\beta} \eta((n+2)\beta + s), \frac{g}{\beta} \right\rangle ds - \int_{0}^{\beta} \left\langle T(\beta - s) \eta((n-1)\beta + s), \frac{g}{\beta} \right\rangle ds \right| \\ &\leq v_{3,2}(h_{i}, g, \beta) + \epsilon + 3e^{3\rho\beta} C L \|g\|\beta + (e^{3\rho\beta} - 1) C K \|g\| + 4e^{3\rho\beta} \sigma, \end{aligned} \tag{29}$$

where  $v_{3,2}$  is given by (24) and we estimated the last two terms of the first inequality similarly to (28).

Now assume that  $|\Delta_n| \le Q_1(g,\beta)$  and  $|\Delta_{n+1}| > Q_1(g,\beta)$ . Then Algorithm 2 returns  $\mathfrak{t}_j = (n+2)\beta$  and  $\mathfrak{f}_j(g) = e^{3\rho\beta}F_{n+3} - F_n$ . We then have

$$\begin{aligned} &|\mathfrak{f}_{j}(g) - \langle h_{j}, g \rangle| \\ &\leq \left| \int_{0}^{\beta} \left\langle T(\beta - s) h_{j} e^{3\rho\beta} \phi((n+3)\beta + s - t_{j}), \frac{g}{\beta} \right\rangle ds - \langle h_{j}, g \rangle \right| \\ &+ \epsilon + 3e^{3\rho\beta} CL \|g\|\beta + (e^{3\rho\beta} - 1)CK \|g\| + 4e^{3\rho\beta} \sigma, \end{aligned}$$

where  $|\int_0^\beta \langle T(\beta-s)h_j e^{3\rho\beta}\phi((n+3)\beta+s-t_j), \frac{g}{\beta}\rangle ds - \langle h_j, g \rangle| = v_{3,3}(h_j, g, \beta)$  is given by (24).

Case 2. The *j*-th burst is in  $[(n+1)\beta, (n+2)\beta)$ , but  $\langle h_j, g \rangle$  it is not detected. If the *j*-th burst occurred in  $[(n+1)\beta, (n+2)\beta)$  but was not detected by Algorithm 2, we use the fact that  $e^{2\rho\beta}F_{n+2} - F_n$  is small to show that  $\langle h_j, g \rangle \approx 0$ .

$$\begin{split} &e^{2\rho\beta}F_{n+2}-F_n\\ &=\int_0^\beta \left\langle T(\beta-s)h_je^{2\rho\beta}\phi((n+2)\beta+s-t_j),\frac{g}{\beta}\right\rangle\!ds\\ &+\sum_{\tau_i< n\beta}\int_0^\beta \left\langle T(\beta-s)f_i(e^{2\rho\beta}\phi((n+2)\beta+s-\tau_i)-\phi(n\beta+s-\tau_i)),\frac{g}{\beta}\right\rangle\!ds\\ &+e^{2\rho\beta}\int_0^\beta \left\langle T(\beta-s)\eta((n+2)\beta+s),\frac{g}{\beta}\right\rangle\!ds-\int_0^\beta \left\langle T(\beta-s)\eta(n\beta+s),\frac{g}{\beta}\right\rangle\!ds+\alpha_n'' \end{split}$$

where  $\alpha_n'' = e^{2\rho\beta} \nu \left( (n+3)\beta, \frac{g}{\beta} \right) - e^{2\rho\beta} \nu \left( (n+2)\beta, \frac{T^*(\beta)g}{\beta} \right) - \nu \left( (n+1)\beta, \frac{g}{\beta} \right) + \nu \left( n\beta, \frac{T^*(\beta)g}{\beta} \right)$ . Now we estimate  $|\langle h_j, g \rangle|$ :

$$\begin{aligned} \left| \langle h_{j}, g \rangle \right| \\ &\leq \left| -\int_{0}^{\beta} \left\langle T(\beta - s)h_{j}e^{2\rho\beta}\phi((n+2)\beta + s - t_{j}), \frac{g}{\beta} \right\rangle ds \right| \\ &+ \left| \int_{0}^{\beta} \left\langle T(\beta - s)h_{j}e^{2\rho\beta}\phi((n+2)\beta + s - t_{j}), \frac{g}{\beta} \right\rangle ds - \langle h_{j}, g \rangle \right| \\ &\leq \left| -\int_{0}^{\beta} \left\langle T(\beta - s)h_{j}e^{2\rho\beta}\phi((n+2)\beta + s - t_{j}), \frac{g}{\beta} \right\rangle ds + (e^{2\rho\beta}F_{n+2} - F_{n}) \right| \\ &+ \left| F_{n} - e^{2\rho\beta}F_{n+2} \right| + v_{2,2}(h_{j}, g, \beta) \\ &\leq \epsilon + 2e^{2\rho\beta}CL\|g\|\beta + (e^{2\rho\beta} - 1)CK\|g\| \\ &+ 4e^{2\rho\beta}\sigma + 2e^{\rho\beta}Q_{1}(g, \beta) + v_{2,2}(h_{j}, g, \beta) \end{aligned}$$
(30)

where we have used  $\left|e^{\rho\beta}F_{n+2} - F_{n+1}\right| \le Q_1(g,\beta), \left|e^{\rho\beta}F_{n+1} - F_n\right| \le Q_1(g,\beta)$ , and estimated the term  $\left|-\int_0^\beta \left\langle T(\beta-s)h_je^{2\rho\beta}\phi((n+2)\beta+s-t_j), \frac{g}{\beta}\right\rangle ds + (e^{2\rho\beta}F_{n+2} - F_n)\right|$  as in (28). The theorem is proved.

🕅 Birkhäuser

15 Page 20 of 24 A. Aldroubi et al.

## 4 Simulation

In order to evaluate the performance of our algorithms, we apply them to the following specific IVP:

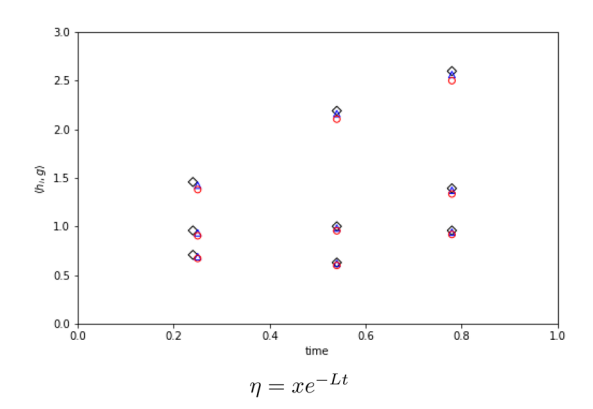
$$\begin{cases} \dot{u}(t) = u(t) + \sum_{i=1}^{\infty} h_i e^{-\rho(t-t_i)} \chi_{[t,\infty)}(t) + \eta \\ u(0) = 0 \end{cases}$$

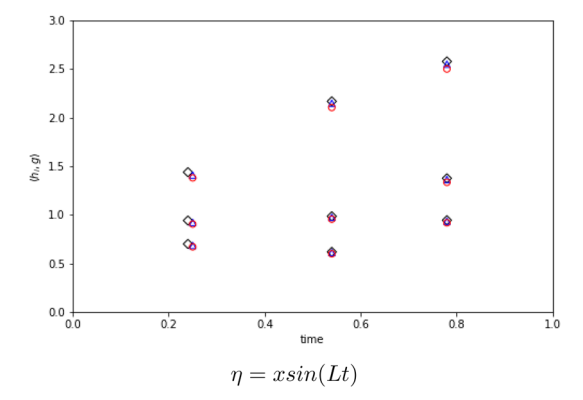
with  $h_1(x) = 3\sin(x)$ ,  $h_2(x) = 2.5\cos(x)$ ,  $h_3(x) = x + 2$ ,  $x \in [0, 1]$ ,  $t_1 = 0.25$ ,  $t_2 = 0.54$ ,  $t_3 = 0.78$ ,  $t \in [0, 1]$ , and one of the two different types of background sources:  $n = xe^{-Lt}$  or  $n = x\sin(Lt)$ .

Let  $g_1(x) = 1$ ,  $g_2(x) = x$ , and  $g_3(x) = x^2$  be the sensor functions and compute the ground truth  $\langle h_i, g_j \rangle$  for i, j = 1, 2, 3. In the simulation, we let  $\rho = 1, L = 10^{-2}$  and the noise level  $\sigma = 10^{-3}$ . The goal is to find the burst times  $\{0.25, 0.76, 1.1\}$  and compare the output  $f_i(g_j)$  with the ground truth  $\langle h_i, g_j \rangle$  (i, j = 1, 2, 3) for different time steps  $\beta = 0.015$  and  $\beta = 0.01$ , respectively. We acquire the measurements (7) and use the algorithm in Sect. 3.1. The results are shown in Fig. 2.

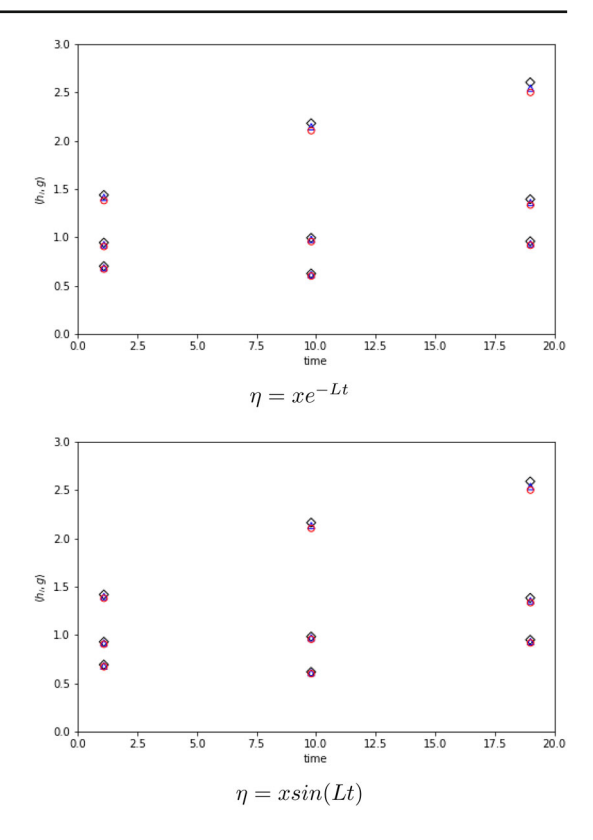
To test the algorithms for the model in Sect. 3.2, we use the same burst and sensor functions. We also test on the same background sources and let  $L=10^{-2}$ . But here

Fig. 2 Plot for the bursts: model with  $\phi(t) = e^{-t}$ ,  $L = 10^{-2}$  and  $\sigma = 10^{-3}$ . The results for  $h_i$  lie in the i-th column. Red circles stand for the ground truth  $\langle h_i, g_j \rangle$ , black squares stand for the output  $\mathfrak{f}_i(g_j)$  when  $\beta = 0.015$  and blue triangles stand for the output  $\mathfrak{f}_i(g_j)$  when  $\beta = 0.01$ .





**Fig. 3** Plot for the bursts: model with  $\phi(t) = \frac{1}{2}(e^{-2t} + e^{-t})$ ,  $L = 10^{-2}$  and  $\sigma = 10^{-3}$ . The results for  $h_i$  lie in the i-th column. Red circles stand for the ground truth  $\langle h_i, g_j \rangle$ , black squares stand for the output  $\mathfrak{f}_i(g_j)$  when  $\beta = 0.015$  and blue triangles stand for the output  $\mathfrak{f}_i(g_j)$  when  $\beta = 0.01$ 



we let  $\phi(t) = \frac{1}{2}(e^{-2t} + e^{-t})$ , thus  $0 < \phi(t) \le e^{-t}$ . For other parameters, we let  $t_1 = 1.1$ ,  $t_2 = 9.8$ ,  $t_3 = 19$ , D = 8.6 and  $\sigma = 10^{-3}$  ( $\epsilon < \sigma$ ). The goal is still to find out the bursts and compare the output with the ground truth for  $\beta = 0.015$  and  $\beta = 0.01$ , respectively. We utilize the algorithm in Sect. 3.2 and the results are shown in Fig. 3.

In Figs. 2 and 3, we plot estimates and ground truth in the same figure. The test shows that our algorithms can find out all bursts and the error gets smaller when the time step  $\beta$  gets shorter. To gain deeper insight into the impact of parameters  $\beta$ , L and  $\sigma$  on our algorithm, we conducted simulations on the model with  $\phi(t) = e^{-t}$  where we varied one parameter and fixed others. In our simulation, we evaluated the accuracy of the estimates of  $\langle h_i, g_2 \rangle$  by calculating the relative error:

$$\frac{\sqrt{\sum_{i=1}^{3} \left| \left\langle h_i, g_2 \right\rangle - \mathfrak{f}_i(g_2) \right|^2}}{\sqrt{\sum_{i=1}^{3} \left| \left\langle h_i, g_2 \right\rangle \right|^2}}.$$

In Fig. 4, we plot the relation between the errors on  $\langle h_i, g_2 \rangle$  and the sampling time step  $\beta$  by fixing the Lipschitz constant of the background source L = 0.01 and the

15 Page 22 of 24 A. Aldroubi et al.

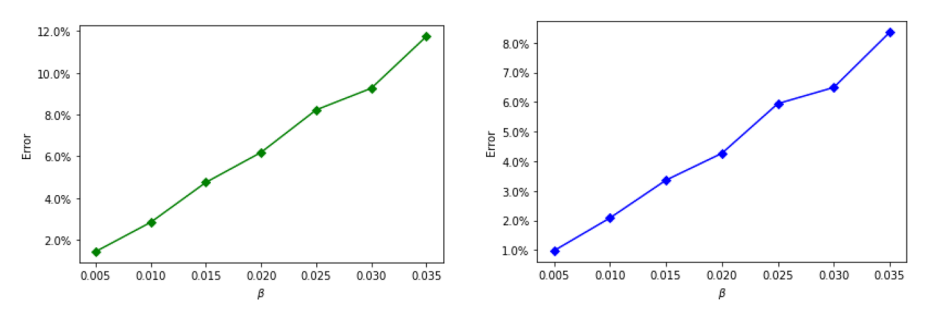


**Fig. 4** The error estimate of  $\langle h_i, g_2 \rangle$   $vs. \beta$ :  $L = 10^{-2}$ ,  $\sigma = 10^{-3}$ . The background sources are  $\eta(x, t) = xe^{-Lt}$  and  $\eta(x, t) = x\sin(Lt)$  for the first and second columns, respectively

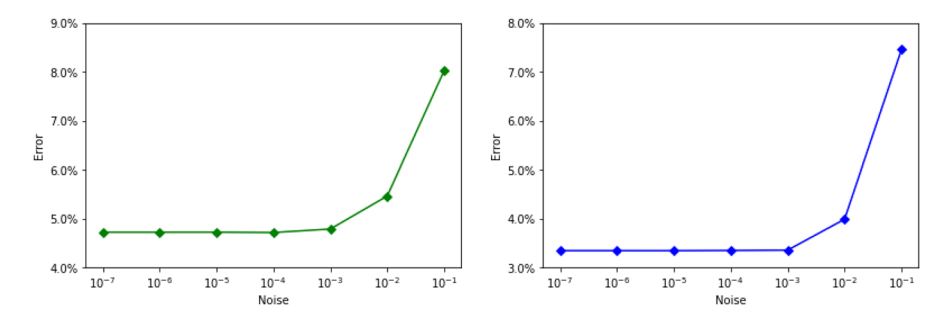
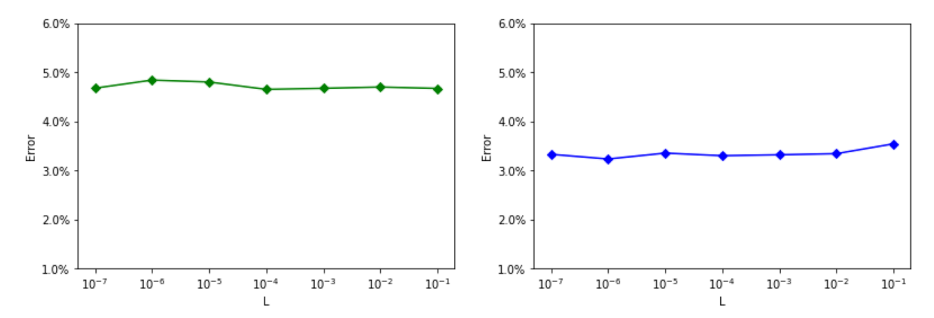


Fig. 5 The error estimate of  $\langle h_i, g_2 \rangle$  vs. Noise:  $L = 10^{-2}$ ,  $\beta = 0.015$ . The background sources are  $\eta(x,t) = xe^{-Lt}$  and  $\eta(x,t) = x \sin(Lt)$  for the first and second columns, respectively



**Fig. 6** The error estimate of  $\langle h_i, g_2 \rangle$  vs. L:  $\beta = 0.015$ ,  $\sigma = 10^{-3}$ . The background sources are  $\eta(x, t) = xe^{-Lt}$  and  $\eta(x, t) = x\sin(Lt)$  for the first and second columns, respectively

noise level  $\sigma = 10^{-3}$ . The results indicate that the error is very low when  $\beta$  is sufficiently small, which demonstrates the accuracy of our algorithm. Additionally, the error appears to grow linearly as  $\beta$  gets bigger.

In Fig. 5, we plot the relation between the errors and the noise level  $\sigma$  by fixing the time step  $\beta$  and the Lipschitz constant L. We notice that in this case the noise level has little influence on the error when it is less than  $10^{-3}$ . When the standard deviation of the additive noise is  $\sigma = 10^{-1}$ , it constitutes roughly 10% of the signal values. Consequently, the error is primarily determined by the additive noise rather

than the time step  $\beta$ , and the Lipschitz constant L of the underlying background  $\eta$ . This phenomenon accounts for the sudden spikes in the relative recovery error.

In Fig. 6, we vary the Lipschitz constant L and fix  $\beta$  and  $\sigma$ . The test shows that for this IVP the error is almost independent of the variance of the Lipschitz constant when  $L < 10^{-1}$ .

**Acknowledgements** The authors of the paper were supported in part by the collaborative NSF Grant DMS-2208030 and DMS-2208031.

**Data availability** The data that support the findings of this study are available from the corresponding author, Le Gong, upon reasonable request.

#### References

- Abdollahpour, M.R., Khedmati, Y.: g-duals of continuous g-frames and their perturbations. Results Math. 73, 152 (2018). (15)
- Aceska, R., Kim, Y.H.: Scalability of frames generated by dynamical operators. Front. Appl. Math. Stat. 3, 22 (2017)
- Aceska, R., Petrosyan, A., Tang, S.: Multidimensional signal recovery in discrete evolution systems via spatiotemporal trade off. Sampl. Theory Signal Image Process. 14, 153–169 (2015)
- Aguilera, A., Cabrelli, C., Carbajal, D., Paternostro, V.: Dynamical sampling for shift-preserving operators. Appl. Comput. Harmon. Anal. 51, 258–274 (2021)
- Aldroubi, A., Davis, J., Krishtal, I.: Dynamical sampling: time-space trade-off. Appl. Comput. Harmon. Anal. 34, 495–503 (2013)
- Aldroubi, A., Davis, J., Krishtal, I.: Exact reconstruction of signals in evolutionary systems via spatiotemporal trade-off. J. Fourier Anal. Appl. 21, 11–31 (2015)
- Aldroubi, A., Gröchenig, K., Huang, L., Jaming, P., Krishtal, I., Romero, J.L.: Sampling the flow of a bandlimited function. J. Geometr. Anal. 31, 9241–9275 (2021)
- Aldroubi, A., Huang, L., Kornelson, K., Krishtal, I.A.: Predictive algorithms in dynamical sampling for burst-like forcing terms. arXiv:2109.00623 (2021)
- Aldroubi, A., Huang, L., Krishtal, I., Ledeczi, A., Lederman, R.R., Volgyesi, P.: Dynamical sampling with additive random noise. Sampl. Theory Signal Image Process. 17, 153–182 (2018)
- Aldroubi, A., Huang, L.X., Petrosyan, A.: Frames induced by the action of continuous powers of an operator. J. Math. Anal. Appl. 478, 1059–1084 (2019)
- 11. Aldroubi, A., Krishtal, I.: Krylov subspace methods in dynamical sampling. Preprint
- Aldroubi, A., Krishtal, I.: Krylov subspace methods in dynamical sampling. Sampl. Theory Signal Image Process. 15, 9–20 (2016)
- Bownik, M., Iverson, J.W.: Multiplication-invariant operators and the classification of LCA group frames. J. Funct. Anal. 280, 108780 (2021). (59)
- Cabrelli, C., Molter, U., Paternostro, V., Philipp, F.: Dynamical sampling on finite index sets. J. Anal. Math. 140, 637–667 (2020)
- Cheng, C., Jiang, Y., Sun, Q.: Spatially distributed sampling and reconstruction. arXiv:1511.08541 (2015)
- Christensen, O., Hasannasab, M.: Frames, operator representations, and open problems. In: The Diversity and Beauty of Applied Operator Theory, Vol. 268 of Oper. Theory Adv. Appl., pp. 155–165. Cham, Birkhäuser/Springer (2018)
- Christensen, O., Hasannasab, M., Philipp, F.: Frame properties of operator orbits. Math. Nachr. 293, 52–66 (2020)
- Corso, R.: Orbits of bounded bijective operators and Gabor frames. Ann. Mat. Pura Appl. 4(200), 137–148 (2021)
- Díaz Martín, R., Medri, I., Molter, U.: Continuous and discrete dynamical sampling. J. Math. Anal. Appl. 499, 125060 (2021). (19)
- Engel, K.-J., Nagel, R.: One-Parameter Semigroups for Linear Evolution Equations, Vol. 194 of Graduate Texts in Mathematics. Springer, New York, With contributions by Brendle, S., Campiti, M., Hahn, T., Metafune, G., Nickel, G., Pallara, D., Perazzoli, C., Rhandi, A., Romanelli, S., Schnaubelt, R. (2000)

15 Page 24 of 24 A. Aldroubi et al.

 Kasumov, Z.A., Shukurov, A.S.: On frame properties of iterates of a multiplication operator. Results Math. 74, 84 (2019). (8)

- Murray-Bruce, J., Dragotti, P.L.: Estimating localized sources of diffusion fields using spatiotemporal sensor measurements. IEEE Trans. Signal Process. 63, 3018–3031 (2015)
- Murray-Bruce, J., Dragotti, P.L.: A sampling framework for solving physics-driven inverse source problems. IEEE Trans. Signal Process. 65, 6365–6380 (2017)
- Ranieri, J., Chebira, A., Lu, Y.M., Vetterli, M.: Sampling and reconstructing diffusion fields with localized sources. In: Acoustics, Speech and Signal Processing (ICASSP), 2011 IEEE International Conference on, pp. 4016–4019 (2011)
- 25. Tang, S.: System identification in dynamical sampling. Adv. Comput. Math. 43, 555–580 (2017)
- Ulanovskii, A., Zlotnikov, I.: Reconstruction of bandlimited functions from space-time samples. J. Funct. Anal. 280, 108962 (2021). (14)
- Zhang, Q., Liu, B., Li, R.: Dynamical sampling in multiply generated shift-invariant spaces. Appl. Anal. 96, 760–770 (2017)

Springer Nature or its licensor (e.g. a society or other partner) holds exclusive rights to this article under a publishing agreement with the author(s) or other rightsholder(s); author self-archiving of the accepted manuscript version of this article is solely governed by the terms of such publishing agreement and applicable law

## Terms and Conditions

Springer Nature journal content, brought to you courtesy of Springer Nature Customer Service Center GmbH ("Springer Nature").

Springer Nature supports a reasonable amount of sharing of research papers by authors, subscribers and authorised users ("Users"), for small-scale personal, non-commercial use provided that all copyright, trade and service marks and other proprietary notices are maintained. By accessing, sharing, receiving or otherwise using the Springer Nature journal content you agree to these terms of use ("Terms"). For these purposes, Springer Nature considers academic use (by researchers and students) to be non-commercial.

These Terms are supplementary and will apply in addition to any applicable website terms and conditions, a relevant site licence or a personal subscription. These Terms will prevail over any conflict or ambiguity with regards to the relevant terms, a site licence or a personal subscription (to the extent of the conflict or ambiguity only). For Creative Commons-licensed articles, the terms of the Creative Commons license used will apply.

We collect and use personal data to provide access to the Springer Nature journal content. We may also use these personal data internally within ResearchGate and Springer Nature and as agreed share it, in an anonymised way, for purposes of tracking, analysis and reporting. We will not otherwise disclose your personal data outside the ResearchGate or the Springer Nature group of companies unless we have your permission as detailed in the Privacy Policy.

While Users may use the Springer Nature journal content for small scale, personal non-commercial use, it is important to note that Users may not:

- 1. use such content for the purpose of providing other users with access on a regular or large scale basis or as a means to circumvent access control;
- 2. use such content where to do so would be considered a criminal or statutory offence in any jurisdiction, or gives rise to civil liability, or is otherwise unlawful;
- 3. falsely or misleadingly imply or suggest endorsement, approval, sponsorship, or association unless explicitly agreed to by Springer Nature in writing;
- 4. use bots or other automated methods to access the content or redirect messages
- 5. override any security feature or exclusionary protocol; or
- 6. share the content in order to create substitute for Springer Nature products or services or a systematic database of Springer Nature journal content.

In line with the restriction against commercial use, Springer Nature does not permit the creation of a product or service that creates revenue, royalties, rent or income from our content or its inclusion as part of a paid for service or for other commercial gain. Springer Nature journal content cannot be used for inter-library loans and librarians may not upload Springer Nature journal content on a large scale into their, or any other, institutional repository.

These terms of use are reviewed regularly and may be amended at any time. Springer Nature is not obligated to publish any information or content on this website and may remove it or features or functionality at our sole discretion, at any time with or without notice. Springer Nature may revoke this licence to you at any time and remove access to any copies of the Springer Nature journal content which have been saved.

To the fullest extent permitted by law, Springer Nature makes no warranties, representations or guarantees to Users, either express or implied with respect to the Springer nature journal content and all parties disclaim and waive any implied warranties or warranties imposed by law, including merchantability or fitness for any particular purpose.

Please note that these rights do not automatically extend to content, data or other material published by Springer Nature that may be licensed from third parties.

If you would like to use or distribute our Springer Nature journal content to a wider audience or on a regular basis or in any other manner not expressly permitted by these Terms, please contact Springer Nature at